# Liquid-phase synthesis and application of monolithic porous materials based on organic-inorganic hybrid methylsiloxanes, crosslinked polymers and carbons

**Kazuyoshi KANAMORI**

Department of Chemistry, Graduate School of Science, Kyoto University, Kitashirakawa, Sakyo-ku, Kyoto 606-8502, Japan

Tel/Fax: +81-75-753-7673

E-mail: kanamori@kuchem.kyoto-u.ac.jp

Keywords: organic-inorganic hybrid; aerogel and xerogel; phase separation; controlled/living radical polymerization; crosslinked polymer; activated carbon

## Abstract

Our recent progress in porous materials based on organic-inorganic hybrids, organic crosslinked polymers, and carbons is summarized. Flexible aerogels and aerogel-like xerogels with the polymethylsilsesquioxane (PMSQ) composition are obtained using methyltrimethoxysilane (MTMS) as the sole precursor. Preparation process and the flexible mechanical properties of these aerogels/xerogels are overviewed. As the derivative materials, hierarchically macro- and mesoporous PMSQ monoliths and marshmallow-like soft and bendable porous monoliths prepared from dimethyldimethoxysilane (DMDMS)/MTMS co-precursors have been obtained. Organic crosslinked polymer monoliths with well-defined macropores are also tailored using gelling systems of vinyl monomers under controlled/living radical polymerization. The obtained polymer monoliths are carbonized and activated into activated carbon monoliths with well-defined pore properties. The activated carbon monoliths exhibit good

electrochemical properties as the monolithic electrode. Some possibilities of applications for these porous materials are also discussed.

## 1. Introduction

The phenomenal development of porous materials through sol-gel chemistry has unlimitedly extended available pore characteristics and chemical compositions. In the conventional sol-gel process, metal alkoxide undergoes hydrolysis and polycondensation to yield desirable forms of gels, such as particles, films and monoliths, during which pore structure is induced in many cases. Mesoporous materials with ordered pore alignments are representatives among products obtained by such process [1]. Hydrolyzed species are self-organized to form three-dimensional (3-D) networks by condensation around the "soft template" or assembly of the structure-directing agent (SDA), typically surfactant molecules, in this case. Even without inducing a specific structure, porous materials can be obtained. Before the dawning of alkoxy-derived sol-gel process, Kistler has invented the imaginative method to remove the pore liquid from the inorganic and organic gels without causing serious shrinkage and cracking by using a supercritical fluid in 1931 [2]. The most part of the pores, initially filled by the pore liquid in the wet gels, survived even after drying. Since the resultant porous materials naturally possess higher porosity compared to those dried under an evaporative condition, he coined the term "aerogel" for these materials. The typical silica aerogels available today exhibit unique pore characteristics such as high porosity (> 90 %) and uniform mesopores (typically 20−50 nm), which allow aerogels to offer unique properties such as low refractive index, high visible-light transparency, and very low thermal conductivity [3,4]. Despite the unique properties, silica aerogels are not widely used due to their extremely poor mechanical properties. Our effort to obtain organic-inorganic hybrid aerogels and xerogels with improved mechanical properties will be described later (Section 2).

In order to tailor larger pores such as submicrons and microns, the phase-separation method is suitable [5,6]. Inorganic oxides such as silica, alumina, titania, zirconia and

siloxane-based organic-inorganic hybrid systems are applicable to this method, in which hydrolyzed and polymerizing species will be destabilized in the aqueous solution containing polar solvent, water-soluble polymer, or surfactant. The thermodynamic instability introduces the formation of characteristic bicontinuous structure in the submicron or micron scale. This type of materials with well-defined macropores takes advantages in fast fluid transport with a low pressure drop because these macropores with relatively high porosity (typically 50−80 %) are 3-D continuous throughout the material. Separation media for high-performance liquid chromatography (HPLC) are primal application for these materials utilizing this advantage [7].

In the present review, we will mainly focus on the new flexible aerogels based on organic-inorganic hybrid networks as well as on the new macroporous crosslinked polymers prepared by controlled/living radical polymerization accompanied by phase separation. Some possible applications are also mentioned.

## 2 Flexible methylsiloxane aerogels and hierarchically porous monoliths

### 2.1 Chemistry of organotrialkoxysilanes [6,8]

A lot of difference should be emphasized in the trifunctional organotrialkoxysilane-derived sol-gel systems from the well-known tetraalkoxysilane-based systems. Inductive and steric effects are the two major factors that influence the reactivity of alkoxysilanes the most. Compared to tetraalkoxysilanes such as tetramethoxysilane (TMOS), alkyltrialkoxysilanes in general show higher reactivity in acid-catalyzed hydrolysis. The rapid first step of hydrolysis includes the protonation of oxygen in the alkoxy groups. Since the less electronegative alkyl group (compared to alkoxy groups) allows more electron density on the oxygen in alkoxy groups, the reaction rate will be higher. In the next step, steric hindrance by the alkyl groups influences the effectiveness of nucleophilic attack of water molecules onto the silicon. Longer or bulky substituent tends to retard hydrolysis. The steric effects work in a similar way both for hydrolysis and condensation in acid/base-catalyzed systems because the penta- or hexacorrdinated

transition state appears in each reaction. In the acid-catalyzed polycondensation step, protonated silanol groups make silicon more susceptible to the nucleophilic attack of water. Since the less electronegative alkyl groups increase the electron density on the silicon, the condensation rate in acid-catalyzed systems should be lower than corresponding tetraalkoxysilanes. The important feature of condensates from organotrialkoxysilanes is that acid-catalyzed less-branched condensates more effectively form stable cyclic species represented by 4-membered rings and 8-membered cages [9]. The 4-membered rings turn into 8-membered cages which increase the hydrophobicity and decrease the connectivity of the network. Phase separation is enhanced in such networks and inhomogeneous monolithic gels [10-12], resin precipitates or stable sols will typically form in acid-catalyzed hydrolysis-condensation systems especially in a dilute condition.

In basic media, conversely, hydrolysis of alkyltrialkoxysilanes is slow because the electron density on the silicon is higher and the rate-determining nucleophilic attack of hydroxide ions is retarded. Once alkyltrialkoxysilane molecule undergoes hydrolysis, rapid polycondensation sequentially proceeds in a similar way to chain reactions. When the electrons are withdrawn from the silicon by hydroxyl groups and/or with the next siloxane linkages, the silicon becomes more susceptible to the following condensation reactions. For this reason, base-catalyzed hydrolysis-condensation systems usually lead to precipitates of vigorously-reacted condensates in the solution while a lot of unreacted monomers remain after slow hydrolysis. The base-catalyzed 1-step process therefore is not generally used to produce monolithic gels in organotrialkoxysilane systems, whereas often employed in tetraalkoxysilane-derived silica aerogels because of its convenience and simplicity.

The acid-base 2-step system is often employed to obtain uniform monolithic gels by solving the aforementioned problems in 1-step acid and 1-step base processes. The first hydrolysis in acidic media allows the fast and effective reaction of alkoxide groups into hydroxide groups. The second condensation in basic media enhances polycondensation of hydrolyzed species, extending the branched siloxane networks. In silica aerogels

preparations, the acid-base 2-step systems are preferred to obtain low-density and highly transparent aerogels with distinct colloidal porous structures [13,14]. The 1-step base process is also capable to produce high-quality aerogels though the intrinsic wide size distributions of condensates may be somewhat inferior to obtain high optical properties. The 1-step acid systems are not very suitable for aerogels because the pore liquid in the less-branched polymeric gels is difficult to be removed without contracting the rather weak networks even by the supercritical drying process [3].

## 2.2 Preparation of transparent polymethylsilsesquioxane aerogels

The aforementioned unique properties of silica aerogels are so attractive that many attempts have been made to use silica aerogels for specific applications such as thermal insulators. However, the high process cost arising from supercritical drying and high fragility have prevented from extended applications. In addition, since hydrophilic surfaces of bare silica aerogels are not stable in a humid condition, a hydrophobizing process using a coupling agent such as hexamethyldisilazane (HMDS) is needed [15]. These drawbacks of silica aerogels can be overcome by reinforcing silica aerogels with polymers or by using organotrialkoxysilane as the (co)precursor. The first approach includes modification of silica networks with organic polymers and post treatment of pore surfaces of silica with organic polymers. However, transparency and porosity are partially or completely sacrificed in this approach. For instance, the group of Leventis has been making continuous efforts to obtain mechanically robust aerogels by crosslinking the pore surfaces with organic polymers such as polyurethane and polystyrene [16,17]. While the robustness is considerably improved by the process, optical transparency and porosity are partially lost. The second approach uses trifunctional organoalkoxysilanes which lower crosslinking density and introduces hydrophobicity in the networks. As a result, since hydrophobic condensates become to form, phase separation from polar solvent occurs. The phase separation induces coarse structures typically in micrometers, which causes the Mie scattering in the sample; aerogels turn into opaque. However, the resultant aerogels

can be flexible against compressive and sometimes tensile and shear stresses without deteriorating porosity. Mckenzie [18] and Rao [19] obtained flexible aerogels from tetraethoxysilane (TEOS)/silanol-terminated polydimethylsiloxane (PDMS) and from methyltrimethoxysilane (MTMS), respectively.

Our process for obtaining transparent low-density aerogels and xerogels also uses MTMS as the sole precursor. The ideal chemical formula of the product obtained from MTMS is methylsilsesquioxane (MSQ, $CH_3SiO_{1.5}$), and gels based on the random networks of MSQ should be termed as polymethylsilsesquioxane (PMSQ). To promote the gelation as a self-supporting monolith, we employed an acid-base two-step reaction, in which pH increase is caused by urea, which is a base-releasing agent. In addition, appropriate surfactant is used to suppress macroscopic phase separation which unless induces visible-light scattering and extinguishes transparency. As a typical synthesis, as shown in Figure 1, MTMS is hydrolyzed in a mixture of acetic acid, water, surfactant, and urea under an acid-catalyzed condition at room temperature, and then undergoes polycondensation at mildly elevated temperature (typically 60 °C), where urea is hydrolyzed into ammonia and carbon dioxide to raise solution pH homogeneously. This is a modified two-step process which can be performed as a one-pot reaction. In the conventional acid-base two-step process, an alkoxysilane is hydrolyzed in an acidic solution, followed by the addition of a base solution. The addition of the base solution in the second step may cause local increase of pH which can lead to heterogeneous growth of the condensates, and may disturb reproducibility. On the other hand, the urea-assisted two-step process offers a simple, homogeneous and highly reproducible procedure for the sol-gel materials production. Within our experience, the urea-assisted process gives more transparent aerogels compared to the conventional two-step process even when the same starting composition is used. With appropriate surfactant, such as *n*-hexadecyltrimethylammonium salt (CTAB for bromide and CTAC for chloride) or poly(ethylene oxide)-*block*-poly(propylene oxide)-*block*-poly(ethylene oxide) triblock copolymer, phase separation is effectively suppressed and transparent aerogels can be obtained [20].

The PMSQ aerogels obtained after supercritical drying exhibit similar properties to the carefully-prepared conventional silica aerogels such as low density (< 0.15 g $cm^{-3}$) and high porosity (~ 90 %), and high visible-light transparency (~ 90 % at 550 nm through a 10 mm-thick-equivalent sample) [20-22]. The typical PMSQ aerogels prepared with CTAB consist of a well-defined mesoscopic pore structure with 30−50 nm pores and solid frameworks formed by nano particles (~10 nm in diameter). Since the small-angle X-ray scattering (SAXS) data on the PMSQ aerogels do not show the fractal nature, which is generally observed on silica aerogels [23], a different aggregation mechanism such as microscopic phase separation may be included in the gelation of PMSQ. However, it can be concluded that the structure and properties, except for mechanical properties, of PMSQ aerogels are almost the same as silica aerogels.

### 2.3 Aerogel-like xerogels by ambient pressure drying

The major advantage in PMSQ aerogels is the flexible and elastic nature upon compression. The optimized aerogel can be uniaxially compressed up to 80 % without cracking, followed by recovering its original size and shape upon unloading, showing the sponge-like compression-reexpansion behavior (spring-back). Although some researchers observed spring-back of silica aerogels treated with a hydrophobic coupling agent such as trimethylchlorosilane [24,25], this is the first example showing the large-scale spring-back in a transparent aerogel monolith. This is attributed to the unique structural characteristics in the PMSQ networks; the lower crosslinking density offers softness, the lower residual silanol groups prohibit irreversible shrinkage upon compression, and the highly concentrated methyl groups induce spring-back by repulsing each other. As a whole, the flexible and elastic mechanical property is imparted in the PMSQ aerogels.

It is well recognized that costly supercritical drying is the high barrier for the industrial aerogel production. Much effort has therefore been made to obtain aerogels without relying on supercritical drying. Evaporative drying of precursor wet gels is often called as ambient pressure drying. Translucent hydrophobic silica aerogel granules

prepared by ambient pressure drying can be commercially available; however, virtually no other examples are found in monolithic aerogels with high transparency and porosity. The major reason is that compressive strength of rigid and fragile silica aerogel is lower than the applied compressive stress during ambient pressure drying. The capillary pressure $p$ exerted on evaporation of solvent with surface tension $\gamma$ can be expressed as follows;

$$p = -\frac{2\gamma \cos\theta}{r},$$

where $\theta$ is the contact angle between solid and liquid, and $r$ is the pore radius. From a simple calculation, the capillary pressure reaches > 3 MPa even when apolar organic solvent such as hexane (~ 18 mN m$^{-1}$ at 25 °C) with low surface tension is used to dry a wet gel with pore radius of 10 nm. Since the compressive strength or yield stress at which irreversible shrinkage occurs in silica aerogel is in general in the order of $10^{-1}$ MPa [26,27], the collapse of pore structures is inevitable. In addition, since as-prepared silica gels involve a considering amount of silanol groups, which react with each other to form new siloxane bonds when compressed. This results in irreversible shrinkage as mentioned above during drying. In order to circumvent this undesirable shrinkage, surface modification using a hydrophobic coupling agent, which also imparts stability against humidity as mentioned above, is necessary. In many cases, however, irreversible shrinkage cannot be completely avoided even after the surface modification, resulting in high-density xerogels.

The flexible nature of PMSQ aerogels facilitates elastic deformation during drying. In an optimized condition, the drying gels do not crack owing to the high compressive strength (> 9 MPa) and spring-back to the original size and shape after pores become empty even without the surface modification. Xerogels with almost the same properties as aerogels can be successfully obtained after careful evaporative drying using a drying solvent with low surface tension. Figure 2 compares aerogel obtained by supercritical drying and xerogel by ambient pressure drying prepared with the identical starting composition. The drying solvent used was methylnonafluorobutyl ether, but we

confirmed it is also possible with hexane, cheaper and common organic solvent. Values of bulk density (porosity) and visible-light transmittance are comparable between the aerogel and xerogel as listed in Table 1. We also confirmed thermal conductivity of the PMSQ xerogel is as low as silica aerogel at ambient pressure (~ 13 $mW\,m^{-1}\,K^{-1}$). The PMSQ xerogel tiles with the size of 250 × 250 × 10 $mm^3$ are readily available with a good reproducibility. The more extended applications of the PMSQ xerogels to thermal insulating materials are highly promising when the low-cost industrial production process will be established without using supercritical drying.

## 2.4 Other porous materials derived from the polymethylsilsesquioxane aerogel systems

Utilizing the urea-assisted acid-base two-step process containing surfactant, two other types of porous materials have been derived. The first example is the PMSQ monoliths with well-defined macropores structured by spinodal decomposition [28]. With decreasing surfactant (Pluronic F127 in this case), a transition from transparent mesoporous aerogel to opaque macroporous gels was observed. The important feature in this material is that mesopores around 10 nm in size and 0.2−0.4 $cm^3\,g^{-1}$ in voume with BET specific surface area > 400 $m^2\,g^{-1}$ are involved in the walls (skeletons) of macropores. In our former results on macroporous PMSQ monoliths prepared using the one-step strong acid-catalyzed systems [29], the nitrogen adsorption-desorption isotherms are all type I and we did not find any mesopores but only micropores in the macropore skeletons. In the polymeric network resulted from the acid-catalyzed system, together with the relatively high volume fraction of monomers (for the MTMS-methanol-nitric acid aq system, volume fraction of MTMS/(entire sol) is typically ~ 0.7), no mesopores are formed. In a base-catalyzed condensation, on the other hand, highly branched colloid-like polymers form as a result of the more vigorous condensation into more-branched silanol species, resulting in inter-particles mesopores formed in the colloidal networks. To the best of our knowledge, this is the first example on hierarchically porous PMSQ monoliths with

well-defined macropores, and we believe that this system serves as a good basis for the better control of mesopores in PMSQ monoliths, which may lead to applications to separation media with improved performances.

The second example is superflexible porous gels from a mixture of MTMS and dimethyldimethoxysilane (DMDMS) [30]. With increasing DMDMS/MTMS molar ratio, though the gels become opaque due to the enhanced hydrophobicity of the networks, resultant gels become more and more flexible and bendable (Figure 3a). The stress upon 80 % compression can be down to *ca.* 0.05 MPa as shown in Figure 3b, which is 1/100 of the MTMS-derived aerogel. These "marshmallow-like" methylsiloxane gels with typical bulk density ~ 0.10 g $cm^{-3}$ can be obtained via ambient pressure drying, and can be subjected to repetitive wetting and drying. Since these bendable gels exhibit good sound absorption properties, applications to high-performance acoustic insulator can be expected.

## 3 Porous organic crosslinked polymer and carbon monoliths

### 3.1 Porous materials from organic polymer gel systems

Porous organic crosslinked polymers are fascinating materials which can be used for separation media, catalyst supports, and carbon sources. In particular, the polymers applied to chromatographic separation media are often called as "polymer monoliths" and mainly prepared using free radical polymerization of monomers containing multiple vinyl groups in a solvent [31,32]. Co-precursor systems consisting of mono-vinyl and di-vinyl compounds such as styrene-divinylbenzene are often employed. Monolithic separation media especially for high molecular weight compounds such as proteins and polypeptides are successful applications because of the presence of micrometer-sized macropores and of the absence of mesopores. In another case, addition-condensation reaction systems of, for instance, resorcinol-formaldehyde (RF), phenol-formaldehyde (PF) and melamine-formaldehyde (MF) are widely studied to obtain monolithic porous polymers [33,34]. Aerogels obtained from RF, MF or other similar systems are particularly attracting attention because these aerogels can be converted to high-surface-area carbon

aerogels by carbonization in an inert atmosphere followed by chemical/physical activation [34,35]. The carbon aerogels are regarded as the promising candidates for electrodes of batteries and electric double-layer capacitors [36].

Our interest in porous crosslinked polymers was originated when we were working on monolithic silica columns for HPLC. While silica columns suffer from dissolution in high pH in aqueous media, crosslinked polymers derived from vinyl monomers are stable in all pH ranges. The silica monoliths obtained by the phase separation method have been proven to show high performance because the monoliths with a well-defined micrometer-sized bicontinuous structure allow fast and neat liquid transport with a low pressure drop [37]. However, polymer monoliths were facing on difficulties in controlling pore properties, *e.g.* pore size and pore volume, which are major parameters in determining separation performances.

The reaction mechanism in free radical polymerization is predominantly responsible for the lack of controllability of pores in polymer monoliths. In the free radical polymerization mechanism, remarkably unstable and reactive free radicals generated from initiator such as 2,2'-azobisisobutylonitrile (AIBN) and benzoyl peroxide (BPO) cleave the double bond in vinyl monomers, generating monomer radicals. The monomer radicals are also significantly reactive and several parallel reactions including propagation, chain transfer and termination occur in an uncontrolled way. In the crosslinking systems, hence, the monomers once started to react will grow in a large size by intra- or intermolecular crosslinking within a short time, resulting in formation and segregation of "microgels" or globules from the solvent. Since the length scale of the microgels is in the order of micrometers, macropores in-between microgels are stochastically formed in the course of gelation. In such systems, fine control of the macropores is appreciably difficult.

In controlled/living radical polymerization (CRP) [38], undesirable chain transfer and termination reactions are highly suppressed by employing a chemical agent (X) which reversibly attaches to the growing end (P·) and stabilizes it as the "domant" (P−X). The domant and dissociated states (P· + X) are in equilibrium with considerably low radical

concentrations, that is, the equilibrium is mostly balanced on the former (Figure 4). By applying energy for dissociation by heat or light, the equilibrium moves to the latter, during which monomer is inserted to forward the propagation reaction. The undesired chain transfer and termination reactions are highly restricted by the low radical concentration, resulting in polymeric products with a narrow molecular weight distribution (= $M_w/M_n$, where $M_n$ and $M_w$ stand for number-average molecular weight and weight-average molecular weight, respectively). Since the growing end is still active or "living" when all the monomers are consumed, well-defined polymers with unique structures such as block and graft copolymers are readily obtained by appending different monomer(s) to the reacted system. Several types of CRP are proposed based on different reaction mechanisms [39-43]. Versatility of applicable monomers and reaction conditions (temperature, atmosphere, *etc*.) are dependent on the mechanisms.

In the crosslinking systems reacted by living polymerization, more homogeneous and uniform networks are reported to form [44,45]. Conversion of the vinyl groups gradually increases with reaction time, and crosslinking density also increases with conversion, leading to the homogeneous gel. The living character offers the narrow molecular weight distribution, sufficient chain/network relaxation, and reactant diffusion in the system. These aspects avoid the formation of microgels, leading to the more homogeneous networks. Also in our experience, free radical polymerization of divinylbenzene initiated by AIBN gives heterogeneous gels in the order of micrometers even in a good solvent (toluene). The homogeneous network formation in CRP is similar to the alkoxy-derived silica sol-gel systems, in which macroscopic phase separation *generally* do not occur and transparent homogeneous gel monoliths are obtained.

### 3.2 Some examples of macroporous crosslinked polymers

While the heterogeneous networks derived by free radical polymerization are utilized to prepare macroporous "polymer monoliths" as mentioned above, we employed CRP to induce spinodal decomposition in the gelling networks and prepare well-defined

macroporous monoliths with controllable porosity. Since it is not possible to induce any structures finer than the heterogeneity of the networks, pore formation by spinodal decomposition in free radical polymerization systems is generally impossible. In our case, spinodal decomposition is induced in a homogeneous network under the co-presence of nonreactive chain polymer, which induces entropy-driven instability with the progress of polymerization of monomer(s) and do not participate in the network.

As the typical starting composition, divinylbenzene (DVB), 1,3,5-trimethylbenzene (good solvent for DVB and poly(divinylbenzene) (PDVB)) and nonreactive polymer such as PDMS to induce phase separation, are mixed with an initiator/promoter system of CRP. In the case of nitroxide-mediated polymerization (NMP), AIBN or BPO and commercially-available stable free radical 2,2,6,6-tetramethyl-1-piperidinyloxy (TEMPO) are used as the initiator/promoter system. The organotellurium-mediated living radical polymerization (TERP) system uses ethyl-2-methyl-2-butyltellanyl propionate (BTEE) with/without the radical initiator. The mixture undergoes CRP at elevated temperatures at 70−125 °C depending on the CRP system, resulting in well-defined macroporous PDVB monoliths as shown in Figure 5. The macroporous morphology coarsens with increasing amount of PDMS (from a to d), and the macropore size and volume are independently controlled by changing the starting composition, which had been difficult by conventional free radical polymerization. In addition, smaller pores in the nanometer scale (with a wide size distribution up to *ca.* 100 nm) are found inside the macropore skeletons by the nitrogen adsorption-desorption measurement. The monoliths therefore possess hierarchically pore structures with relatively high specific surface area (~ 600−800 $m^2 g^{-1}$). So far, we have obtained several macroporous crosslinked polymers from DVB [46,47], glycerol 1,3-dimethacrylate (GDMA) [48,49], trimethylolpropane trimethacrylate (Trim) [49] and *N*,*N*'-methylenebisacrylamide (BIS) [50] in the CRP systems such as NMP, TERP, and atom transfer radical polymerization (ATRP). The latter two affords reactions at lower temperatures, and TERP proceeds even without a radical initiator. We have also confirmed that the similar porous materials can be obtained by anionic polymerization,

which also behaves as living polymerization, using such as *n*-butyl lithium or potassium *tert*-butoxide. It can therefore be concluded that the formation of network without heterogeneity coarser than the desired structure is the most crucial factor to obtain macroporous materials by the phase separation method. The gradual or stepwise increase of crosslinking density with conversion/reaction time is the essential feature to obtain homogeneous networks. Inorganic, organic, and their hybrid macroporous materials based on the well-defined bicontinuous structure are therefore readily obtained in the stepwise polymerization systems such as so-called sol-gel, addition-condensation [51], and polyaddition [52]. In spite of the technical importance, macroporous vinyl polymers with the bicontinuous structure have not been reported so far for this reason. In Figure 6, differences in the network and pore formations in free radical polymerization and CRP are summarized by comparative depictions. Note again that free radical polymerization induces heterogeneity even without a counter polymer, while spinodal decomposition can be induced in the homogeneous network derived by CRP under the co-presence of a counter polymer.

Although all of these examples are initiated and reacted by applying heat to the system, we have confirmed that similar pore formations occur in the systems initiated by ultraviolet (UV) light irradiation. The UV-initiating system can offer position-selective formation of porous parts for catalytic reaction, separation and purification in microfluidic channels of lab-on-a-chip, *etc* [53-55].

### 3.3 Carbonization and application

The obtained PDVB monoliths can be converted to carbonaceous materials by carbonization in an inert atmosphere with preserving the macroporosity and monolithicity as shown in Figure 7 [56,57]. Carbonization of as-prepared PDVB monoliths decreased the sample weight in 10−20 % by the pyrolysis of the networks, and specific surface area drastically increased (~ 1500 $m^2 g^{-1}$) by carbonization at > 900 °C. The turbostratic structure, which is the disordered stacking of 2-D polycyclic aromatic (graphene) sheets, is

proposed from the XRD patterns with broad peaks at around 23 and 43 deg, and the structure has been developed mainly at 600−800 °C confirmed by FTIR. Activation under 10 % carbon dioxide in nitrogen further increases specific surface area above 2300 $m^2 g^{-1}$. Sulfonation of as-prepared PDVB monoliths before carbonization suppresses the excess pyrolysis and carbon yield increases from 10−20 % to 30−40 %, because aromatic rings are bridged with sulfonyl groups at around 300 °C in the course of carbonization [58]. At the same time, the pyrolyzing networks are mechanically reinforced by the sulfonyl bridges, which preserve nanometer-scaled pores in the original skeletons from shrinkage. Hence, carbonization/activation of the sulfonated PDVB networks allows development of micropores with preserving macro- and mesoporosity and monolithicity, resulting in hierarchically porous carbon monoliths with trimodal sizes of pores and increased specific surface area.

The (activated) carbon monoliths are also obtained by carbonization of macroporous polymer monoliths [51], employing sacrificial template [59,60], and removing silica phase from carbon/silica composites [61]. We have also successfully obtained macroporous polysilsesquioxane monoliths from phenylene- and biphenylene-brided alkoxysilanes, which can be converted to a carbon/silica nanocomposite monolith when heat-treated in inert atmosphere below 1200 °C [62] and silicon carbide (SiC) monoliths when heat-treated above 1300 °C [63,64]. The nano-sized silica phase in the resultant carbon/silica nanocomposite can be removed using aqueous basic solution to increase micropores, typically ~ 1.5 nm [65], which we call the “nano-phase extraction” technique. Carbon monoliths with ~ 2000 $m^2 g^{-1}$ can be obtained by this method. Liu *et al.* reported that ordered mesoporous silica in addition to carbon can be prepared by the removal of carbon phase by calcination in air from carbon-silica nanocomposite, which is obtained by parallel sol-gel reactions of silica and PF materials [66,67].

The activated carbon monoliths prepared from PDVB were electrochemically tested as a monolithic polarizable electrode. As shown in Figure 8, by cyclic voltammetry (CV) and galvanostatic charge-discharge measurements, relatively high specific capacitance was

obtained such as 175 F $g^{-1}$ at 5 mV $s^{-1}$ (CV) and 206 F $g^{-1}$ at 500 mA $g^{-1}$ (charge-discharge) in 2 M aqueous $H_2SO_4$ using a three-electrode cell [68]. Compared to other reported capacitance values of monolithic electrodes, the obtained capacitance values are sufficiently high [69-71]. While conventional electrodes are typically fabricated in pellets or slurries from composites of polymer binders, carbon black as conducting agent and activated carbons as active material, the monolithic electrode consists only of the active material with the hierarchical porosity. Therefore the effective diffusion and permeation of the electrolyte are expected and electric conductivity of the monoliths is relatively high owing to the continuous skeletal structure. In addition, since the chemical and mechanical durability are also expected to be higher in the monolithic electrode, applications are highly promising to electrode for electric double-layer capacitors with a good reproducibility and cycle performance. Also, it is expected in the future works that the pseudocapacitance by doping of heteroatoms such as nitrogen or by inclusion of transition metal oxides in the carbon matrix will further increase the performances.

## 4 Conclusions and future perspectives

In the present review, the pore formations in the organotrialkoxysilane-derived sol-gel system (see also our recent reviews [6,72]) and in the controlled/living radical polymerization (CRP) of vinyl compounds in solvent are summarized. As well known in silica sol-gel systems, the well-defined macroporous structure is developed as a result of spinodal decomposition during transitions to gel in both systems. The activated carbon monoliths with high specific surface area and multimodal porosity are readily obtained by carbonization and activation of the crosslinked polymers under an inert atmosphere. Possibility of applications to electrochemical devices has also been demonstrated.

We are expecting CRP systems can be extended to various porous materials with wide pore properties and materials shapes (particles, films, monoliths, *etc.*) because we believe the homogeneous network formation by CRP is capable of inducing a variety of porous structures possibly with the multiple hierarchy. In addition-condensation systems

such as resorcinol-formaldehyde (RF), which is also capable of forming homogeneous networks, some exciting results such as ordered mesoporous materials are already obtained. The similar development can be expected in CRP systems of vinyl monomers.

By adequately controlling reaction conditions and phase separation in organotrialkoxysilane-derived sol-gel systems, organic-inorganic hybrid aerogels with high visible light transparency and low density have been obtained. Although there have been a lot of effort to impart flexibility or to reinforce the fragile silica networks by employing co-precursor systems of tetraalkoxysilane and organotrialkoxysilanes or diorganodialkoxysilanes, or by introducing organic polymers, transparency and/or porosity are sacrificed in the resultant aerogels. We successfully demonstrate that it is remarkably beneficial to employ methyltrimethoxysilane (MTMS) as the sole precursor to increase mechanical flexibility and strength with preserving silica aerogel-like unique characteristics. In addition, aerogel-like xerogels can be obtained by simple evaporative drying of solvent in the atmospheric condition owing to the high flexibility and strength. Extended applications to such as high-performance thermal insulators are promising when the simplification of these xerogels production will be steadily achieved in an industrial production scale.

## Acknowledgements

The author wishes to thank all the coworkers who supported him, gave critical ideas to him, and contributed to his experimental works. Most of the names of the coworkers appear as the co-authors in the references.

Financial supports such as Grant-in-Aid for Scientific Research and Global COE Program from Ministry of Education, Culture, Sports, Science and Technology (MEXT) Japan and Japan Society for the Promotion of Science (JSPS) are acknowledged.

## References


[1] Soler-Illia GJAA, Sanchez C, Lebeau B, Patarin J (2002) Chem Rev 102:4093-4138

[2] Kistler SS (1931) Nature 127:741

[3] Hüsing N Schubert U (1998) Angew Chem Int Ed 37:22-45

[4] Pierre AC, Pajonk GM (2002) Chem Rev 102:4243-4265

[5] Nakanishi K (1997) J Porous Mater 4:67-112

[6] Kanamori K, Nakanishi K (2011) Chem Soc Rev 40:754-770

[7] Nakanishi K, Tanaka N (2007) Acc Chem Res 40:863-873

[8] Brinker CJ, Scherer GW (1990) Sol-Gel Science: The Physics and Chemistry of Sol-Gel Processing. Academic Press, San Diego

[9] Baney RH, Itoh M, Sakakibara A, Suzuki T (1995) Chem Rev 95:1409-1430

[10] Dong H, Lee M, Thomas RD, Zhang Z, Reidy RF, Mueller DW (2003) J Sol-Gel Sci Technol 28:5-14

[11] Dong H, Brook MA, Brennan JD (2005) Chem Mater 17:2807-2816

[12] Dong H, Zhang Z, Lee M-H, Mueller DW, Reldy RF (2007) J Sol-Gel Sci Technol 41:11-17

[13] Tillotson TM, Hrubesh LW (1992) J Non-Cryst Solids 145:44-50

[14] Emmerling A, Petricevic R, Beck A, Wang P, Scheller H, Fricke (1995) J Non-Cryst Solids 185:240-248

[15] Yokogawa H, Yokoyama M (1995) J Non-Cryst Solids 186:23-29

[16] Leventis N, Sotiriou-Leventis C, Zhang G, Rawashdeh A-MM (2002) Nano Lett 2:957-960

[17] Ilhan UF, Fabrizio EF, McCorkle L, Scheiman DA, Dass A, Palczer A, Meador MAB, Johnston JC, Leventis N (2006) J Mater Chem 16:3046-3054

[18] Kramer SJ, Rubio-Alonso F, Mackenzie JD (1996) Mater Res Soc Symp Proc 435:295-300

[19] Rao AV, Bhagat SD, Hirashima H, Pajonk GM (2006) J Colloid Interface Sci 300:279-285

[20] Kanamori K, Aizawa M, Nakanishi K, Hanada T (2007) Adv Mater 19:1589-1593
[21] Kanamori K, Aizawa M, Nakanishi K, Hanada T (2008) J Sol-Gel Sci Technol 48:172-181
[22] Kanamori K, Nakanishi K, Hanada T (2009) J Ceram Soc Jpn 117:1333-1338
[23] Schaefer DW, Keefer KD (1986) Phys Rev Lett 56:2199-2202
[24] Prakash SS, Brinker CJ, Hurd AJ, Rap SM (1995) Nature 374:439-443
[25] Schwertfeger F, Schmidt DFM (1998) J Non-Cryst Solids 225:24-29
[26] Parmenter KE, Milstein F (1998) J Non-Cryst Solids 223:179-189
[27] Alaoui AH, Woignier T, Scherer GW, Phalippou J (2008) J Non-Cryst Solids 354:4556-1561
[28] Kanamori K, Kodera Y, Hayase G, Nakanishi K, Hanada T (2011) J Colloid Interface Sci 357:336-344
[29] Kanamori K, Yonezawa H, Nakanishi K, Hirao K, Jinnai H (2004) J Sep Sci 27:874-886
[30] Hayase G, Kanamori K, Nakanishi K (2011) J Mater Chem, 21:17077-17079
[31] Gusev I, Huang X, Horváth C (1999) J Chromatogr A 855:273-290
[32] Svec F (2010) J Chromatogr A 1217:902-924
[33] Pekala RW, Alviso CT, Kong FM, Hulsey SS (1992) J Non-Cryst Solids 145:90-98
[34] Al-Muhtaseb SA, Ritter JA (2003) Adv Mater 15:101-114
[35] Hanzawa Y, Kaneko K, Pekala RW, Dresselhaus MS (1996) Langmuir 12:6167-6169
[36] Frackowiak E, Béguin F (2001) Carbon 39:937-950
[37] Guiochon G (2007) J Chromatogr A 1168:101-168
[38] Braunecker WA, Matyjaszewski K (2007) Prog Polym Sci 32:93-146
[39] Matyjaszewski K, Xia J (2001) Chem Rev 101: 2921-2990
[40] Hawker CJ, Bosman AW, Harth E (2001) Chem Rev 101:3661-3688
[41] Kamigaito M, Ando T, Sawamoto M (2001) Chem Rev 101:3689-3745
[42] Moad G, Rizzardo E, Thang SH (2005) Aust J Chem 58:379-410
[43] Yamago S (2009) Chem Rev 109:5051-5068

[44] Norisuye T, Morinaga T, Tran-Cong-Miyata Q, Goto A, Fukuda T, Shibayama M (2005) Polymer 46:1982-1994
[45] Yu Q, Zhou M, Ding Y, Jiang B, Zhu S (2007) Polymer 48:7058-7064
[46] Kanamori K, Nakanishi K, Hanada T (2006) Adv Mater 18:2407-2411
[47] Hasegawa J, Kanamori K, Nakanishi K, Hanada T, Yamago S (2009) Macromolecules 42:1270-1277
[48] Kanamori K, Hasegawa J, Nakanishi K, Hanada T (2008) Macromolecules 41:7186-7193
[49] Hasegawa G, Kanamori K, Nakanishi K, Yamago S (2011) Polymer, published online
[50] Hasegawa G, Kanamori K, Nakanishi K, Hanada T, Yamago S (2009) Macromol Rapid Commun 30:986-990
[51] Liang C, Dai S (2009) Chem Mater 21:2115-2124
[52] Tsujioka N, Hira N, Aoki S, Tanaka N, Hosoya K (2005) Macromolecules 38:9901-9903
[53] Yu C, Davey MH, Svec F, Fréchet JMJ (2001) Anal Chem 73:5088-5096
[54] Faure K, Blas M, Yassine O, Delaunay N, Crétier G, Albert M, Rocca J-L (2007) Electrophoresis 28:1668-1673
[55] Proczek G, Augustin V, Descroix S, Hennion M-C (2009) Electrophoresis 30:515-524
[56] Hasegawa J, Kanamori K, Nakanishi K, Hanada T (2010) CR Chimie 13:207-211
[57] Hasegawa G, Kanamori K, Nakanishi K, Hanada T (2010) Carbon 48:1757-1766
[58] Neely JW (1981) Carbon 19:27-36
[59] Taguchi A, Smått J-H, Lindén M (2003) Adv Mater 15:1209-1211
[60] Lee KT, Lytle JC, Ergang NS, Oh SM, Stein A (2005) Adv Funct Mater 15:547-556
[61] Pang J, John VT, Loy DA, Yang Z, Lu Y (2005) Adv Mater 17:704-707
[62] Hasegawa G, Kanamori K, Nakanishi K, Hanada T (2010) Chem Commun 46:8037-8039
[63] Hasegawa G, Kanamori K, Nakanishi K, Hanada T (2010) J Mater Chem 19:7716-7720

[64] Hasegawa G, Kanamori K, Nakanishi K, Hanada T (2010) Chem Mater 22:2541-2547
[65] Hasegawa G, Kanamori K, Nakanishi K, submitted
[66] Liu R, Shi Y, Wan Y, Meng Y, Zhang F, Gu D, Chen Z, Tu B, Zhao D (2006) J Am Chem Soc 128:11652-11662
[67] Wei H, Lv Y, Han L, Tu B, Zhao D (2011) Chem Mater 23:2353-2360
[68] Hasegawa G, Aoki M, Kanamori K, Nakanishi K, Hanada T, Tadanaga K (2011) J Mater Chem 21:2060-2063
[69] Fan L-Z, Hu Y-S, Maier J, Adelhelm P, Smarsly B, Antonietti M (2007) Adv Funct Mater 17:3083-3087
[70] Ruiz V, Blanco C, Santamaría R, Ramos-Fernández JM, Martínez-Escandell M, Sepúlveda-Escribano A, Rodríguez-Reinoso F (2009) Carbon 47:195-200
[71] Carriazo D, Picó F, Gutiérrez MC, Rubio F, Rojo JM, del Monte F (2010) J Mater Chem 20:773-780
[72] Kanamori K (2011) J Ceram Soc Jpn 119:16-22

Table

Table 1 Comparison between supercritically-dried PMSQ aerogel and evaporatively-dried xerogel[a]

| | Bulk density/g cm$^{-3}$ | Porosity/% | Light transmittance[*2]/% |
|---|---|---|---|
| Aerogel | 0.13 | 91 | 89 |
| Xerogel | 0.14 | 90 | 84 |

[a] Starting composition; MTMS 5 mL, 5 mM acetic acid aq 10 mL, CTAB 0.4 g, and urea 3.0 g. [*2]Light transmittance at 550 nm through 10 mm-thick equivalent samples.

## Figure legends

Figure 1 The process for preparing transparent PMSQ monoliths by the modified one-pot 2-step reaction. All the starting materials are mixed in advance to the addition of MTMS. Hydrolysis is catalyzed by acetic acid and polycondensation is by ammonia generated by *in-situ* hydrolysis of urea at > 60 °C. Transparent monolithic gels can be obtained under the co-presence of adequate surfactant. Drying of the resultant monolith either by the supercritical or ambient condition will give aerogel or aerogel-like xerogel monoliths, respectively.

Figure 2 Comparison between supercritically-dried PMSQ aerogel and evaporatively-dried PMSQ xerogel with similar pore properties (see also Table 1).

Figure 3 Flexible methylsiloxane aerogel/xerogel prepared from DMDMS-MTMS co-precursors exhibiting a bendable feature. By increasing the DMDMS ratio, the compressive stress dramatically decreases to *ca*. 1/100 of MTMS-derived aerogels.

Figure 4 General concept of controlled/living radical polymerization; M, P, and X show monomer, polymer, and a chemical agent which attaches the growing end and makes "domant" species (P−X). Monomers are inserted to increase molecular weight on the "activation" of the equilibrium.

Figure 5 Typical macroporous morphologies of PDVB monoliths prepared by NMP. From parts a to d, macropores are coarsened with increasing concentration of PDMS (phase separation inducer). The lower figures obtained by mercury porosimetry demonstrates that only macropore size can be varied with increasing PDMS (from a to d), and only macropore volume can be changed with increasing both PDMS and TMB (solvent) (c, e, and f).

Figure 6 Comparative illustrations showing differences in network and pore formations in free radical and controlled/living radical polymerizations. In the heterogeneous networks derived by free radical polymerization, micrometer-sized pores are stochastically generated as a result of microgel formation. In the more homogeneous networks derived by controlled/living radical polymerization, well-defined and controllable pores are formed through phase separation induced by a non-reactive polymer additive.

Figure 7 Changes in appearance and morphology of PDVB monoliths by sulfonation and carbonization. Well-defined macropores and monolithicity are successfully preserved after carbonization.

Figure 8 Appearance of the typical activated carbon monoliths for monolithic electrode. From electrochemical measurements such as cyclic voltammetry (CV, lower left) and galvanostatic charge-discharge (lower right), the high specific capacitance was confirmed, which, together with the monolithic feature, is advantageous for applications to electric double-layer capacitors.

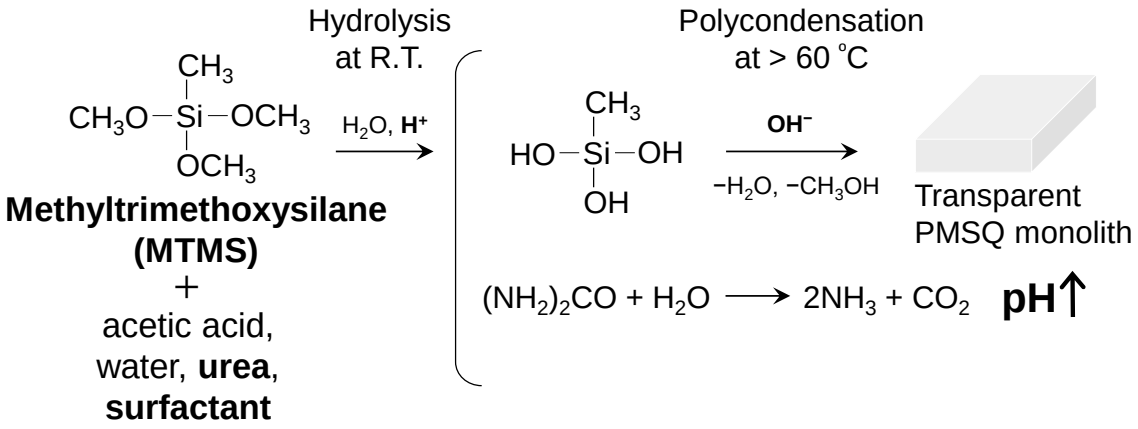


Figure 1

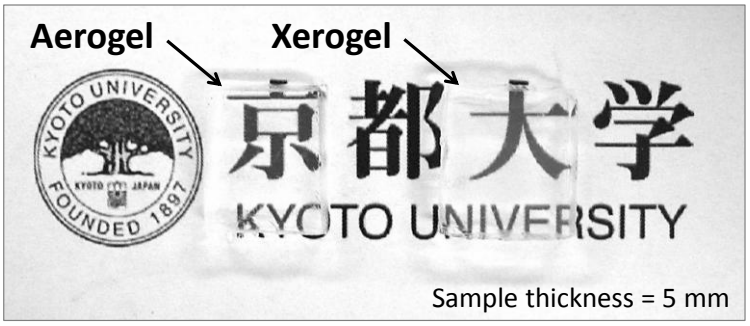


Figure 2

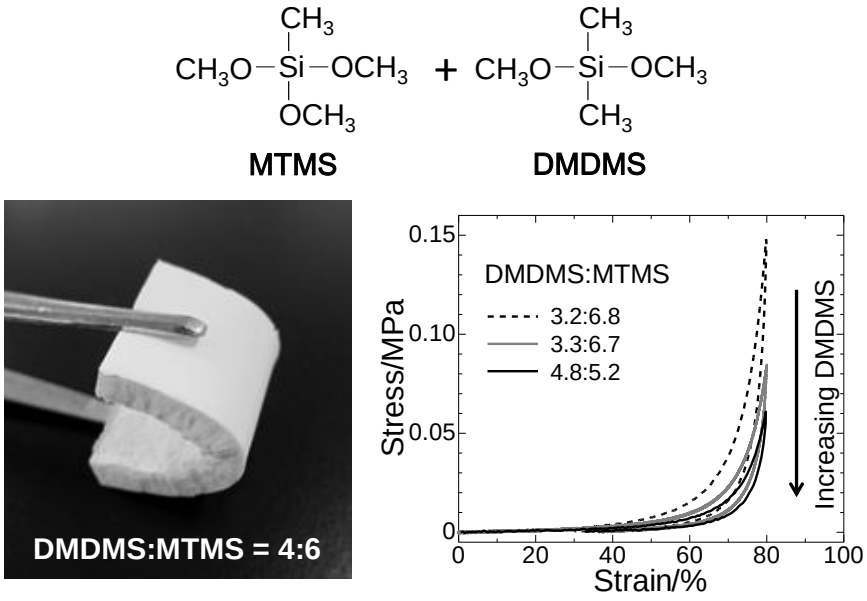


Figure 3

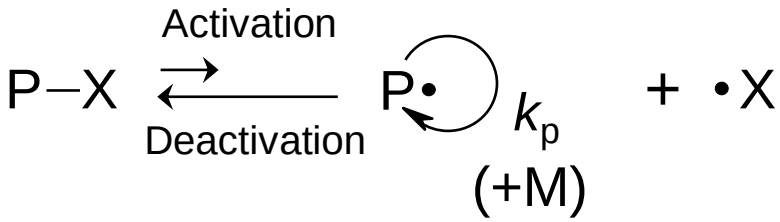


Figure 4

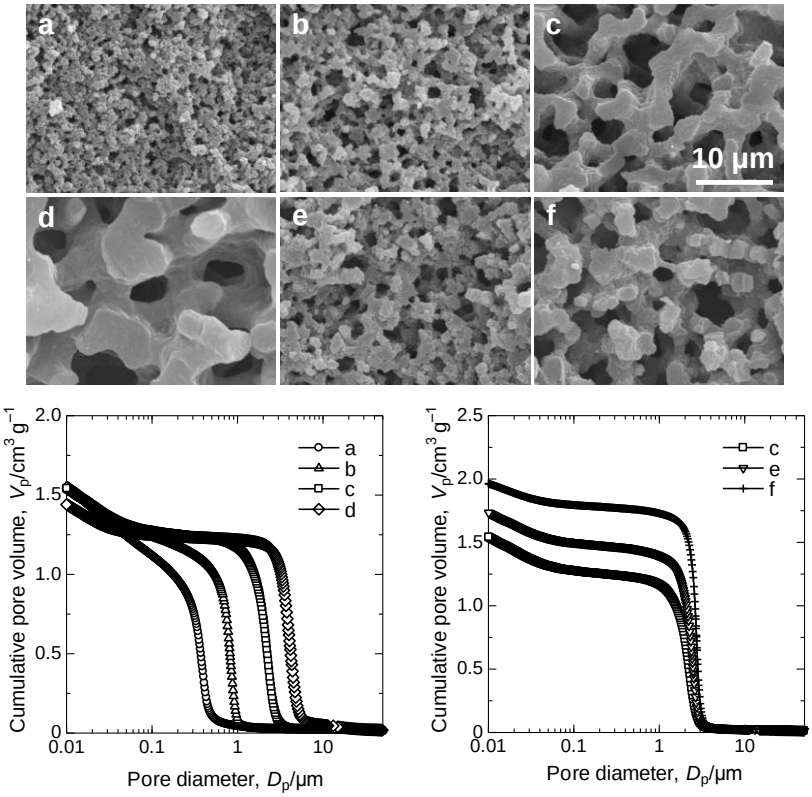


Figure 5

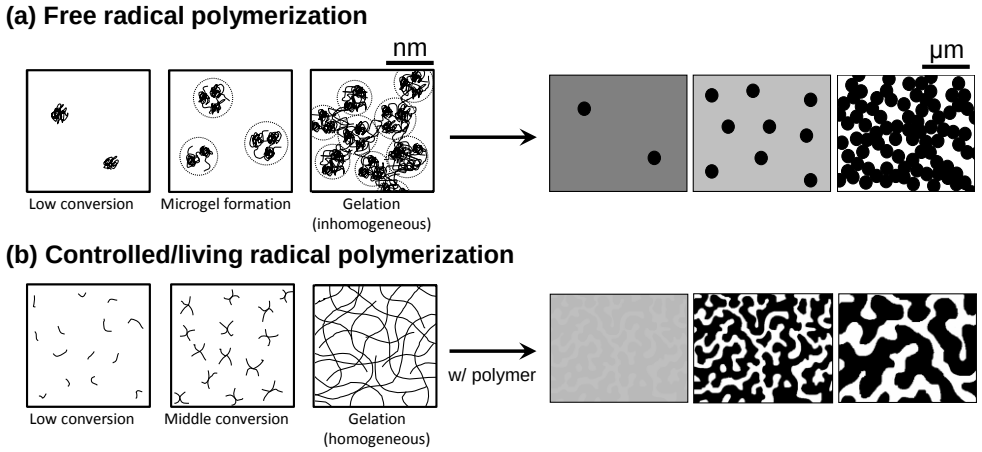


Figure 6

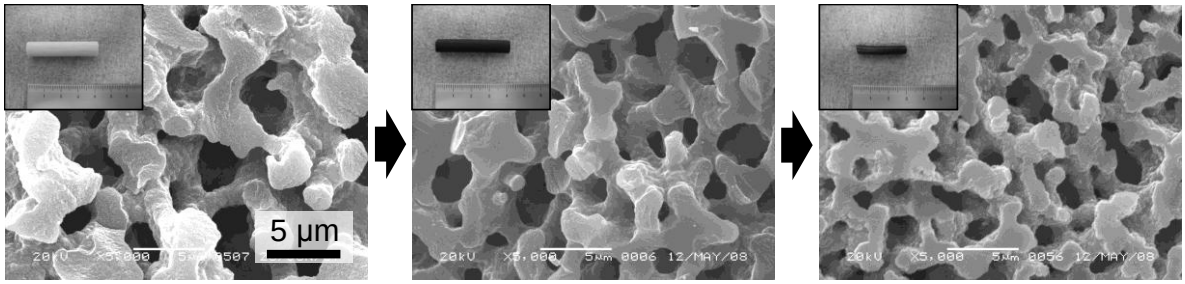


Original PDVB

Sulfonated at 120 ºC with conc. $H_2SO_4$

Carbonized at 800 ºC under $N_2$ atmosphere

Figure 7

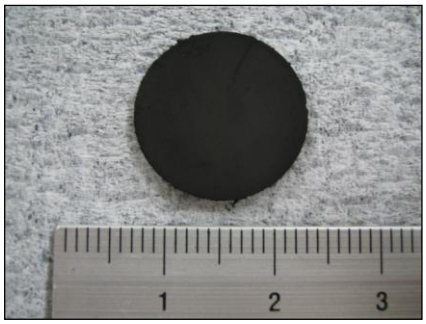

Micro-/meso-/macroporous
Specific surface area : 2420 $m^2\,g^{-1}$
Bulk density : 0.22 $g\,cm^{-3}$

**175 F $g^{-1}$ (at 5 mV $s^{-1}$)**
**206 F $g^{-1}$ (at 500 mA $g^{-1}$)**

*in 2 M $H_2SO_4$ aq, three-electrode cell

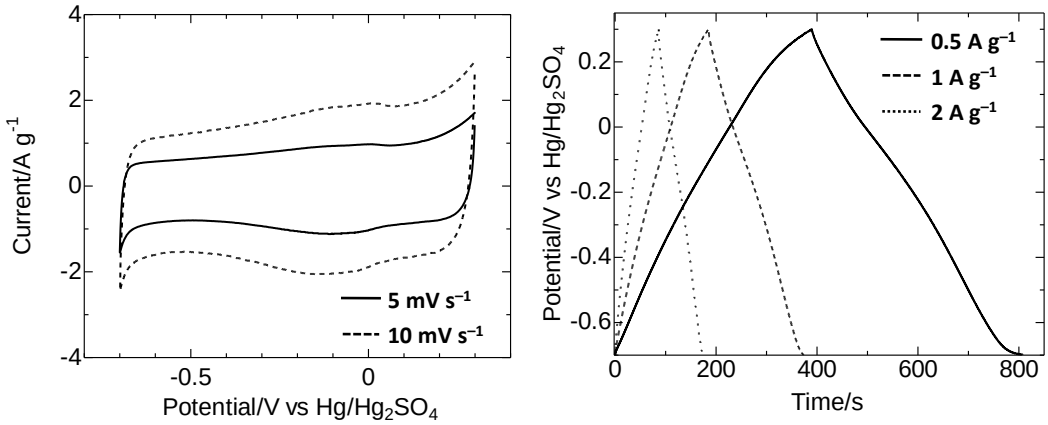


Figure 8